THE EFFECT OF TUBE INTERNAL GEOMETRY ON THE PROPENSITY TO SPONTANEOUS IGNITION IN PRESSURIZED HYDROGEN RELEASE

B P XU[1,2] AND J X WEN[3*]

[1] Centre for Fire and Explosion Studies, Faculty of Engineering, Kingston University
Friars Avenue, London, SW15 3DW, United Kingdom
[2] School of Energy and Power Engineering, Dalian University of Technology, Dalian, China
[3] School of Engineering, University of Warwick, Coventry CV4 7AL, United Kingdom

ABSTRACT

Over recent years, the spontaneous ignition from compressed hydrogen release has attracted considerable attention. Owing to the ultra fast evolution and intrinsic complexities of the flow structures, most previous experimental studies focused on phenomenal observations. Therefore, high resolution CFD approach is often employed to investigate the spontaneous ignition mechanism. Most previous studies on the topic considered compressed hydrogen release via a length of straight tube. However, according to Dryer's [2] experimental findings, the internal geometry of the release tube plays an important role in the occurrence of the spontaneous ignition. In the present study, spontaneous ignition of compressed hydrogen release through a length of tube with different internal geometries is numerically investigated using our previously developed model [6-8, 10-12]. Four types of internal geometry are considered: local contraction, local enlargement, abrupt contraction and abrupt enlargement. It is found that the presence of internal geometries can significantly increase the propensity to spontaneous ignition. Shock reflections from the surfaces of the internal geometries and the subsequent shock interactions further increase the temperature of the combustible mixture at the contact region. The presence of the internal geometry also stimulates turbulence enhanced mixing between the shock-heated air and the escaping hydrogen, resulting in the formation of more flammable mixture. It is also revealed in this study in comparison with backward-facing vertical planes, forward-facing vertical planes are more likely to cause spontaneous ignition by producing the highest heating to the flammable mixture.

Keywords: Spontaneous ignition; Shock reflection; Numerical simulation.

1. INTRODUCTION

As a possible next-generation energy carrier, hydrogen's safe transport and utilization is of particular importance. A potential hazard of such system is the high pressure hydrogen releases which are prone to spontaneous ignition [1-14].

Experimental [2-4] and numerical [5-14] investigations have revealed that a possible mechanism of hydrogen spontaneous ignition is shock-induced diffusion ignition. As compressed hydrogen is suddenly released into the ambient environment, a shock wave is generated ahead of the emerging jet and driven into air. The air behind the shock is heated to a level well above the hydrogen auto-ignition temperature. The shock-heated air exchanges mass and energy with hydrogen at contact region, leading to an ignition under specific release conditions. Most previous experimental studies [2-4] focused on phenomenological observations of pressurized releases through a length of tube. According to these experimental observations, release pressure and length of release tube are two major factors

---

[*]Corresponding author: jennifer.wen@warwick.ac.uk

affecting the occurrence of the spontaneous ignition: a higher release pressure would facilitate the occurrence of ignition by producing a higher shock-heated temperature, while a longer tube would provide a longer mixing time to make ignition more readily happen. Dryer et al. [2] also emphasized the importance of the internal geometry downstream of the burst disk and the multi-dimensional shock formation/reflection/interaction resulting from the rupture process of the bursting disk, and postulated that both factors were responsible for significant mixing occurring at the contact surface.

The majority of the previous numerical studies were concerned with releases through a length of tube with constant cross-section except that Xu et al. [6] numerically investigated the effect of a local contraction inside the release tube on the spontaneous ignition. Their study revealed that a local contraction significantly facilitate the occurrence of spontaneous ignition by producing elevated flammable mixture and enhancing turbulent mixing from shock formation, reflection and interaction. Here our previous study [6] is extended to include more general types of internal geometry: local contraction, local enlargement, abrupt contraction and abrupt enlargement.

2. NUMERICAL METHODS

For details of the numerical methods, the readers should refer to our previous publication [11]. Briefly, an arbitrary Lagrangian and Eulerian (ALE) method [16] is adopted to treat convective terms separately from diffusion terms in the transport equations considering the substantial scale difference between diffusion and advection. A second-order Crank-Nicolson scheme is used for the diffusion terms and the terms associated with pressure wave propagation, a 3rd-order TVD Runge–Kutta method [17] is used to solve the convection terms. For spatial differencing, a 5th-order upwind WENO scheme [15] is used for the convection terms and the 2nd-order central differencing scheme for all the other terms.

A mixture-averaged multi-component approach [18] is used for the molecular transport with consideration of thermal diffusion for non-premixed hydrogen combustion. For autoignition chemistry, Saxena and Williams' detailed chemistry scheme [19] which involves 21 elementary steps among eight reactive chemical species is used. The scheme was previously validated against a wide range of pressures up to 33 bar. It also gave due consideration to third body reactions and the reaction-rate pressure dependent ''fall-off'' behaviour. To deal with the stiffness problem of the chemistry, the chemical kinetic equations are solved by a variable-coefficient ODE solver [20].
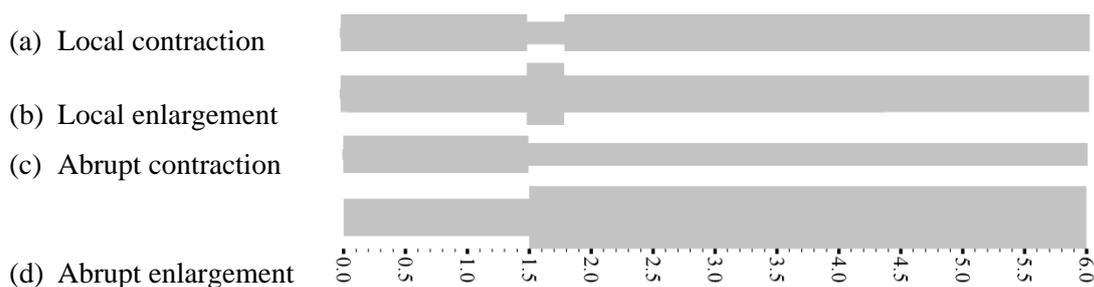
Figure. 1. Release tubes with varied cross-sections.

3. PROBLEM DESCRIPTIONS

Table 1 Computational details

Parameters	Values
Rupture time (µs)	5
Release pressure (bar)	50
Initial temperature (K)	293
Initial diameter of tube (mm)	3
Length of tube (mm)	60
Contraction/expansion ratios	0.6/1.5
Thickness of film(mm)	0.1
Minimum grid spacing (µm)	15
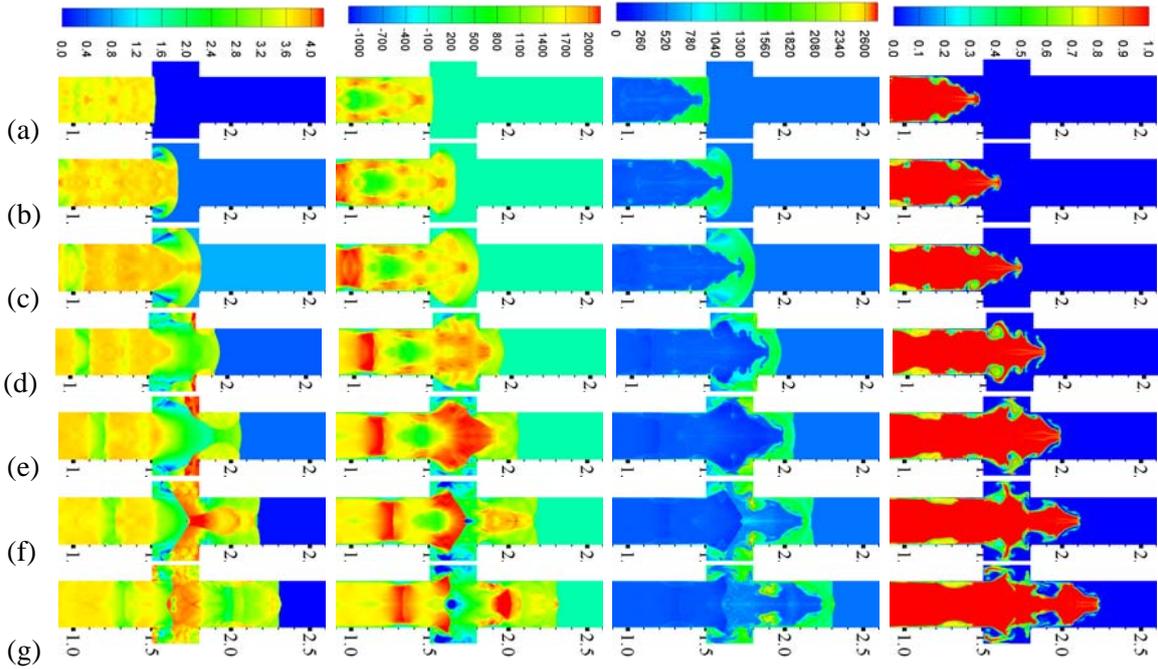
Figure 2. Predicted contours of Logarithm of pressure (bar), axial velocity (m/s), temperature (K) and hydrogen mass fraction listed from the left to right columns respectively at a time interval of 1 µs starting from 13 µs.

It was revealed in our previous study [11] that spontaneous ignition firstly occurs inside release tubes and gradually evolves into a partially pre-mixed flame before jetting out of tube exits. Therefore, the present study is limited to the flow inside the tube. The computational domain is composed of a cylindrical high-pressure vessel of large diameter and a release tube with varied cross-sections as shown in Fig. 1. The pressurized cylinder is set up to be sufficiently large to ensure that pressure drop during simulations does not exceed 3% of the initial pressure. The release tubes have an initial diameter D of 3 mm and a length L of 6 cm. The contraction and expansion ratios are fixed to be 0.6 and 1.5, respectively in this study. The distance of the internal geometries to the rupture plane is chosen as 5 times of the initial diameter to allow the incident shock to reach a nearly constant shock velocity before it transmits into the abrupt change in flow area. The width of the local contraction/enlargement is set to be the tube diameter. Our previous study [11] has revealed that the rupture process of the initial pressure boundary is crucial to the spontaneous ignition. An Iris model [21] was used to simulate the rupture process of the pressure boundary. It assumes that the pressure boundary, which is mimicked by a thin diaphragm with a thickness of 0.1 mm placed at the left plane

of the release tube in the simulations, ruptures linearly from the centre at a finite pre-determined rate as the computations start. To obtain a fast increase rate of the shock velocity, in this study the rupture time, which is the time for a full bore opening of the thin diaphragm, is fixed as 5 µs. The release pressure of 50 bar, which are not sufficiently high to produce a spontaneous ignition for a tube of a constant cross-section, is considered.

All the simulations start from still with the tube filled with ambient air and the pressurized cylinder region with pure pressurized hydrogen separated by a thin diaphragm with a thickness of 0.1 mm. All the wall surfaces are assumed to be non-slip and adiabatic. Non-uniform grids are used for the pressurized cylinder while and uniform grids are used for the tube region. Since flame is firstly initiated at the thin contact region, a very fine grid resolution is required to resolve the species profiles in the ignited flame. Following our previous study [11] a 15 µm grid size is used. The non-uniform grids are clustered around the two ends of the tube and the grid sizes range from 15 µm ~150 µm inside the region of the pressurized cylinder. The total grid points are approximately two millions. The key parameters of the computed release scenarios are summarized in Table 1.

(a) Pressure   (b) Axial velocity

(c) Hydrogen mass fraction   (d) OH mass fraction
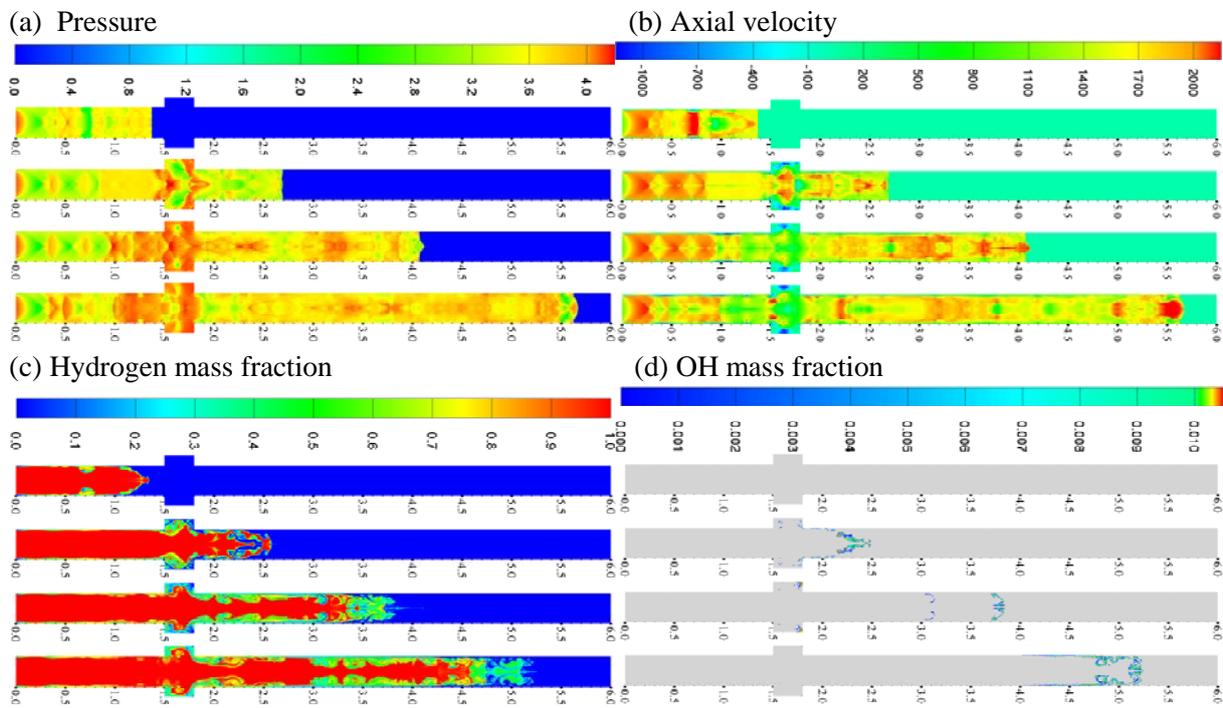
Figure 3. The predicted contours of Logarithm of pressure (bar), axial velocity (m/s), hydrogen mass fraction and OH mass fraction at a time interval of 10 µs starting from 12µs.

Figure 3 shows the predicted contours of pressure, axial velocity, hydrogen mass fraction, OH mass fraction at a time interval of 10 µs starting from 12 µs for the case of local enlargement. As the leading shock wave propagates downstream the expansion, the aforementioned shock reflection and interaction repeat from the tube wall, generating a supersonic jet behind it and creating an intermittent turbulent flow pattern (see Figure 3(a) and 3(b)). The developed turbulent flow significantly enhances the mixing process creating significant amount of partially premixed combustible mixture (see Figure 3(c)). Although the ignition kernels are initiated at the thin contact region, a partially premixed flame quickly develops due to the fast turbulent enhanced mixing. It can be found from Figure 3(d) that there are two major flame regions: one at the front of the contact surface and the other inside the recirculation zone of the local enlargement. The flame inside the recirculation zone is eventually

quenched from the mixing with the cooled hydrogen while the frontal flame grows and is finally extended into the boundary layer (see Figure 3(d).

Figures 4 shows scattered plots of the OH radical mass fraction versus mixture fraction at every computational cell centres for the case of local enlargement. The mixture fraction is defined by

$$f = \frac{\phi Y_{H_2} - Y_{O_2} + Y_{O_2,\text{inf}}}{\phi Y_{H_2,\text{inf}} + Y_{O_2,\text{inf}}} \tag{1}$$

where the mass ratio of oxygen to hydrogen at stoichiometry $\phi = 8$, Y_{H_2} and Y_{O_2} are mass fractions of hydrogen and oxygen respectively, $Y_{O_2,\text{inf}} = 0.23$ and $Y_{H_2,\text{inf}} = 1.0$ are mass fractions at infinity. The stoichiometric mixture fraction is therefore $f_{st} = 0.028$, while for pure air and pure hydrogen the mixture fraction is equal to 0.0 and 1.0 respectively. The scatter of OH mass fraction at t=32 μs is sparser than that at t=22 μs, indicating flame quenching inside the recirculation region during the period. The ignition kernel has a significant thickness in the mixture fraction space spanning from f =0.0 to f =0.08 and the reaction rate peaks at a mixture fraction f_{mr}=0.025 called most reactive mixture fraction slightly deviating from the stoichiometric mixture fraction f_{st} =0.028. From 32μs to 42μs the scattered plot gets denser due to the flame growth. At t=42 μs, OH radical mass fraction still show large scatter owing to the different local flow conditions resulting from the highly turbulent flow.
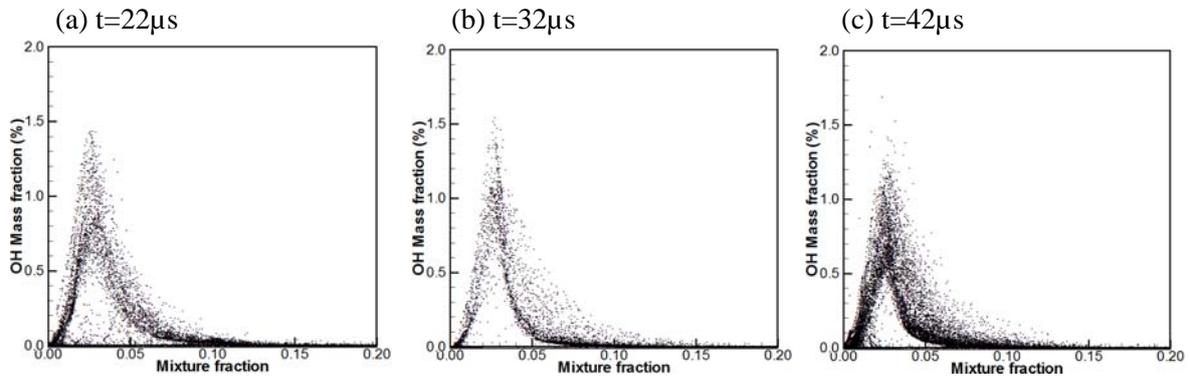
Figure 4. Scattered plots of OH radical mass fraction versus mixture fraction for the case of local enlargement at different release moment.

Figure 5 shows the maximum temperature versus release time for five different internal geometries under the release pressure of 50 bar. The maximum temperature jumps to 1046K at t=0.2 μs after the rupture due to shock heating and then drops to 624K at t=2.3 μs due to flow divergence. After t=2.3 μs it quickly increases again due to the shock reflection. Two spikes at t=6.6 μs and 8.3 μs are caused by shock focusing. For the case with a constant cross-section, it finally stabilizes a value of 1653K from t=13 μs and no ignition occurs. For the cases of local contraction and abrupt contraction, it jumps to 2522K at t=13 μs due to the strong shock reflection from the vertical planes. After the reflection, it decreases to 2377K at t=13.7 μs and then jumps to 3000K due to the ignition at t=14 μs. After the ignition, it fluctuates but still remains at a very high value. In comparison to the case of abrupt contraction there exist more spikes for the case of local contraction after t=20μs due to further shock reflections and focusing resulting from the second abrupt expansion.

For the case with a local enlargement, it jumps to 2715K at t=15.5 μs due to the strong shock reflection from the right vertical plane. After the reflection, it decreases to 1945K at t=16.7 μs and then jumps to 2703K due to the ignition at t=18 μs. After the ignition, it fluctuates but still remains at a very high value. The spikes appearing after the ignition are caused by shock reflections and focusing. For the case with an abrupt enlargement, as the incident shock reaches the abrupt expansion, the

maximum temperature starts to slightly decrease due to flow divergence and then jumps to 2600K at t=18.5 µs due to the shock focusing resulting from shock reflections from the tube wall. The sharp increase in temperature causes an ignition at small regions at the tube axis and the ignited spots quench quickly after t=30 µs.
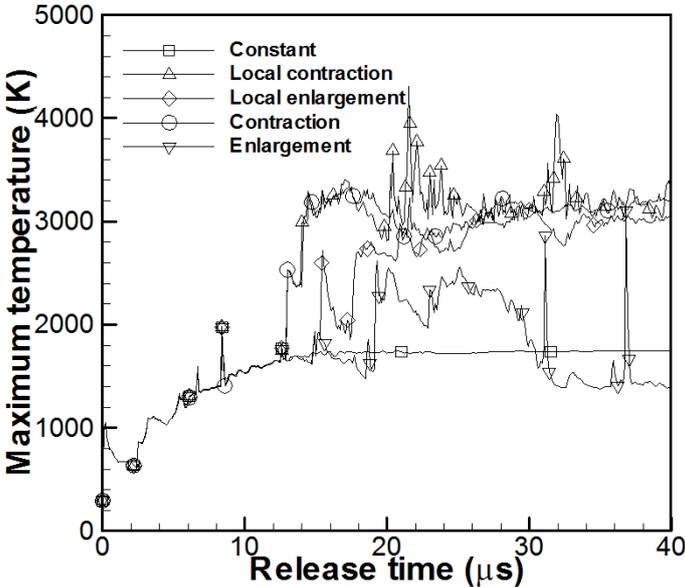
Figure 5. Maximum temperature versus release time for five different internal geometries under the release pressure of 50 bar.
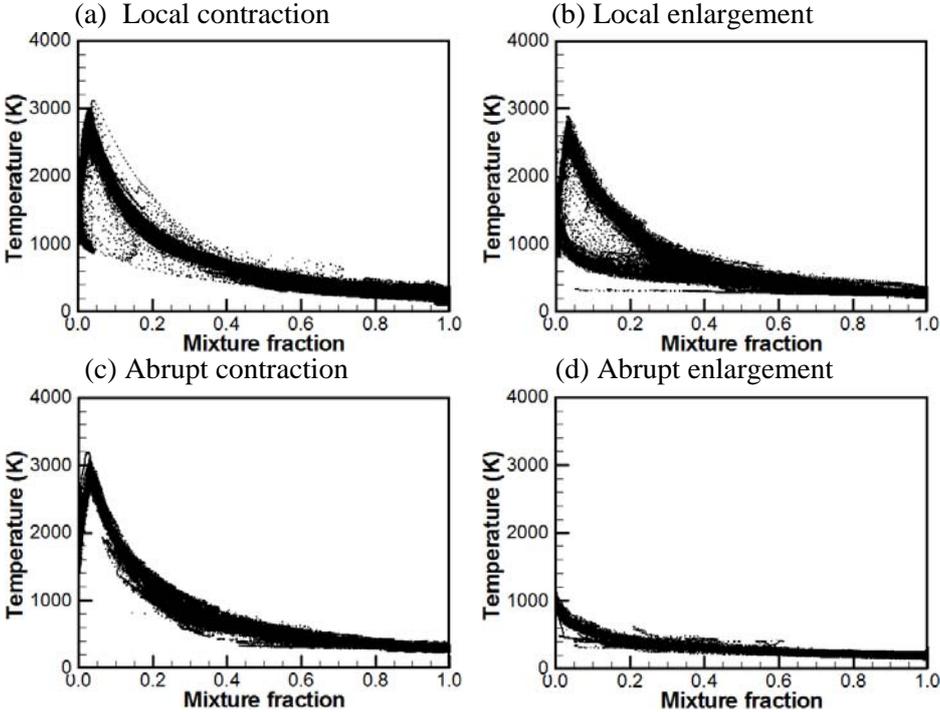
Figure 6. Scattered plots of temperature versus mixture fraction for four different internal geometries under the release pressure of 50 bar at t= 40 µs.

Figure 6 displays scattered plots of temperature versus mixture fraction for four different internal geometries under the release pressure of 50 bar at the t= 40 µs. For the case of local contraction (Figure 5a) the majority of temperature scatter points cluster around the equilibrium line indicating

that the flames almost spread over all the interfaces between hydrogen and shock-heated air; the temperature reaches a peak value of 3000K around the stoichiometric mixture. For the case of local enlargement (Figure 5b) the temperature scatter points cluster around both the equilibrium line and the mixing line, so only part of the interface is ignited. For the case of abrupt contraction (Figure 5c) all the temperature scatter points cluster around the equilibrium line indicating that the flames spread over all the interfaces. For the case of abrupt enlargement (Figure 5d) the temperature scatter points cluster around the mixing line indicating that no flames exist inside the tube.

5. SUMMARY

The effect of tube internal geometry on the spontaneous ignition of pressurized hydrogen release has been investigated by simulating four types of internal geometries i.e. local contraction, local enlargement, abrupt contraction and abrupt enlargement. As the incident shock hit a forward-facing vertical plane, a strong curvilinear reflected shock is generated receding towards the rupture plane. Swept by the reflected shock, the temperature of the flammable mixture at the contact region is elevated. As the planar incident shock passes a backward-facing vertical plane, it quickly diffracts into a semi-spherical shock which is then reflected back from the tube side wall creating shock focusing at the axis of symmetry.

The flow development at the internal geometries is complicated due to shock formation, reflection and interaction. The curvilinear reflected shock converges and reflects from the axis of symmetry creating high-speed jet flows and intermittent flow pattern. Downstream the internal geometries, in addition to the repeating shock reflections between tube wall and the axis, these complex flow developments create a highly turbulent flow significantly distorting the contact region and enhancing its mixing. Although the ignition kernels are initiated at the thin contact region, partially premixed flames quickly develop due to the fast turbulent enhanced mixing. The partially premixed flames are highly distorted by the turbulent flow and overlapped with each other. Flame thickening was also observed due to the merge of thin flames for the cases of local contraction and abrupt contraction.

According to the present study, the internal geometries with a forward-facing vertical plane can significantly increase the propensity to spontaneous ignition by producing elevated flammable mixture and turbulent enhanced mixing. Comparing to the forward-facing vertical plane, the backward-facing vertical plane is less likely to cause spontaneous ignition as the reflected shock from the side wall is relatively weak. These findings have practical applications for hydrogen safety as in practice there are often various fixtures inside the tubes.

REFERENCES

1. Astbury, G.R. and Hawksworth, S.J., Spontaneous ignition of hydrogen leaks: a review of postulated mechanisms, *Int. J Hydrogen Energy*, 32, 2007, pp. 2178-2185.
2. Dryer, F.L., Chaos, M., Zhao, Z., Stein, J.N., Alpert, J.Y. and Homer. C.J., Spontaneous Ignition of Pressurized Releases of Hydrogen and Natural Gas into Air, *Combust. Sci. and Tech.*, 179, 2007, pp. 663-694.
3. Mogi, T., Kim, D., Shiina H. and Horiguchi, S., Self-ignition and explosion during discharge of high-pressure hydrogen, *Journal of Loss Prevention in the Process Industries*, 21, No. 2, 2008, pp. 199-204.
4. Golub, V.V., Baklanov, D.I., Bazhenova, T.V., Bragin, M.V., Golovastov, S.V. Ivanov, M.F., Volodin, V.V., Shock-induced ignition of hydrogen gas during accidental or

technical opening of high-pressure tanks, *Journal of Loss Prevention in the Process Industries*, 21, No. 2, 2008, pp. 185-198.

5. Liu, Y.F., Sato, H., Tsuboi, N., Hjigashino F. and Hayashi, A.K., Numerical simulation on hydrogen fuel jetting from high pressure tank, *Sci. Tech. Energ. Mater.*, 67, 2006, pp. 7-11.

6. Xu, B.P., Wen, J.X., Numerical study of spontaneous ignition in pressurized hydrogen release through a length of tube with local contraction, *Int J Hydrogen Energy* 37(22), 2012, pp. 17571-579.

7. Xu, B.P., Wen, J.X., Dembele, S., Tam, V.H.Y., Hawksworth, S.J., The effect of pressure boundary rupture rate on spontaneous ignition of pressurized hydrogen release, *Journal of Loss Prevention in the Process Industries*, 22, No. 3, 2009, pp. 279-287.

8. Xu, B.P., Hima, L. EL., Wen, J.X. and Tam, V.H.Y., Numerical study of spontaneous ignition of pressurized hydrogen release into air, *Int. J Hydrogen Energy*, 34, 2009, pp. 5954-5960.

9. Yamada, E., Watanabe, S., Hayashi A.K. and Tsuboi, N., Numerical analysis on autoignition of a high-pressure hydrogen jet spouting from a tube, *Proc. Combust. Inst.*, 32, No. 2, 2009, pp. 2363-2369.

10. Xu, B.P., Hima, L.EL., Wen, J.X., Dembele, S., Tam, V.H.Y., Donchev, T., Numerical Study of Spontaneous Ignition of Pressurized Hydrogen Release through a tube into Air, *Journal of Loss Prevention in the Process Industries*, 21, No. 2, 2008, pp. 205-221.

11. Wen, J.X., Xu, B.P., Tam, V.H.Y., Numerical study on spontaneous ignition of pressurized hydrogen release through a length of tube, *Combustion and Flame*, 156, No. 11, 2009, pp. 2173-2189.

12. Xu, B.P.J. Wen, J.X., Tam, V.H.Y. The effect of an obstacle plate on the spontaneous ignition in pressurized hydrogen release: A numerical study, *Int. J Hydrogen Energy*, 36, No. 3, pp. 2637-2644.

13. Bragin, M.V., Molkov, V.V., Physics of spontaneous ignition of high-pressure hydrogen release and transition to jet fire, *Int. J Hydrogen Energy,* 36, No. 3, pp. 2589-2596.

14. Lee, B.J., Jeung, I.S., Numerical study of spontaneous ignition of pressurized hydrogen released by the failure of a rupture disk into a tube, *Int. J Hydrogen Energy*, 34, 2009, pp. 8763-8769.

15. Jiang, G.S., Shu, C.W., Efficient implementation of weighted ENO schemes, *J. Comput. Phys.* , 126, 1996, pp. 202-228.

16. Hirt, C.W., Amsden, A.A., Cook, J.L., Anarbitrary Lagrangian-Eulerian computing method for all flow speeds, *J. Comput. Phys.*, 14, 1974, pp. 227-253.

17. Balsara, D.S., Shu, C.W., Monotonicity prserving weno schemes with increasingly high-order of accuracy, *J. Comput. Phys.*, 160, 2000, pp. 405-452

18. Kee, R.J., Rupley, F.A., Miller, J.A., Chemkin II: a fortran chemical kinetics package for the analysis of gas-phase chemical kinetics. Sandia National Laboratories Report No. SAND89-8009, 1989.

19. Saxena, P. and Williams, F.A. Testing a small detailed chemical-kinetic mechanism for the combustion of hydrogen and carbon monoxide, *Combustion and Flame*, 145, 2006, pp. 316-323.

20. Brown, P.N., Byrne, G.D. and Hindmarsh, A. C., VODE, a Variable-Coefficient ODE Solver, *SIAM J. Sci. Stat. Comput.*, 10, 1989, pp.1038-1051.

21. Goozee, R.J., Jacobs, P.A., Buttsworth, D.R., Simulation of complete reflected shock tunnel showing a vortex mechanism for flow contamination, *Shock waves*, 15, No. 3-4, 2006, pp. 165-176.